


Treating solid tumors with TCR-based chimeric antigen receptor targeting extra domain B-containing fibronectin

Zhijie Zhang,¹ Chang Liu,¹ Muhan Wang,¹ Rongcheng Sun,^{1,2} Zhe Yang,¹ Zhen Hua,¹ Yushuang Wu,² Mengting Wu,² Hang Wang,¹ Wen Qiu,³ Hongping Yin,¹ Meijia Yang ²

To cite: Zhang Z, Liu C, Wang M, *et al.* Treating solid tumors with TCR-based chimeric antigen receptor targeting extra domain B-containing fibronectin. *Journal for ImmunoTherapy of Cancer* 2023;**11**:e007199. doi:10.1136/jitc-2023-007199

► Additional supplemental material is published online only. To view, please visit the journal online (<http://dx.doi.org/10.1136/jitc-2023-007199>).

Accepted 27 July 2023



© Author(s) (or their employer(s)) 2023. Re-use permitted under CC BY-NC. No commercial re-use. See rights and permissions. Published by BMJ.

¹School of Life Science and Technology, China Pharmaceutical University, Nanjing, Jiangsu, China

²Jiangsu Cell Tech Medical Research Institute, Nanjing, Jiangsu, China

³Department of Immunology, Nanjing Medical University, Nanjing, Jiangsu, China

Correspondence to

Dr Hongping Yin;
yinhongping63@163.com

Dr Meijia Yang;
meijia.yang@celltechjs.com

ABSTRACT

Background The suppression of chimeric antigen receptor (CAR) T cells by the tumor microenvironment (TME) is a crucial obstacle in the T-cell-based treatment of solid tumors. Extra domain B (EDB)-fibronectin is an oncofetal antigen expressed on the endothelium layer of the neovasculature and cancer cells. Though recognized as a T cell therapy target, engineered CAR T cells thus far have failed to demonstrate satisfactory in vivo efficacy. In this study, we report that targeting EDB-fibronectin by redirected TCR-CAR T cells (rTCR-CAR) bypasses the suppressive TME for solid tumor treatment and sufficiently suppressed tumor growth.

We generated EDB-targeting CAR by fusing single-chain variable fragment to CD3 ϵ , resulting in rTCR-CAR. Human primary T cells and Jurkat cells were used to study the EDB-targeting T cells. Differences to the traditional second-generation CAR T cell in signaling, immune synapse formation, and T cell exhaustion were characterized. Cytotoxicity of the rTCR-CAR T cells was tested in vitro, and therapeutic efficacies were demonstrated using xenograft models.

Methods

Results In the xenograft models, the rTCR-CAR T cells demonstrated in vivo efficacies superior to that based on traditional CAR design. A significant reduction in tumor vessel density was observed alongside tumor growth inhibition, extending even to tumor models established with EDB-negative cancer cells. The rTCR-CAR bound to immobilized EDB, and the binding led to immune synapse structures superior to that formed by second-generation CARs. By a mechanism similar to that for the conventional TCR complex, EDB-fibronectin activated the rTCR-CAR, resulting in rTCR-CAR T cells with low basal activation levels and increased in vivo expansion.

Conclusion Our study has demonstrated the potential of rTCR-CAR T cells targeting the EDB-fibronectin as an anticancer therapeutic. Engineered to possess antiangiogenic and cytotoxic activities, the rTCR-CAR T cells showed therapeutic efficacies not impacted by the suppressive TMEs. These combined characteristics of a single therapeutic agent point to its potential to achieve sustained control of solid tumors.

WHAT IS ALREADY KNOWN ON THIS TOPIC

⇒ Previous exploration of targeting the extracellular matrix for cancer treatment has included studying the extra domain B (EDB)-fibronectin, a protein with restricted expression pattern in the extracellular matrix of tumor neovasculature. Although therapeutic antibodies and chimeric antigen receptor (CAR) T cells aimed at EDB-fibronectin have been explored, no positive clinical or preclinical outcomes have been achieved thus far.

WHAT THIS STUDY ADDS

⇒ rTCR-CAR T cells targeting EDB-fibronectin significantly reduced the growth of cancer cells with or without EDB-fibronectin. rTCR-CAR T cells targeting EDB-fibronectin bypassed the immune suppressive environment, inhibiting tumor growth by collapsing neovasculature in the tumor tissue.

HOW THIS STUDY MIGHT AFFECT RESEARCH, PRACTICE OR POLICY

⇒ A cellular therapy effective against a wide range of solid tumors or lymphomas may be developed by targeting EDB-fibronectin. This approach provides a safe alternative since the EDB-fibronectin is not expressed in normal tissues. Further, it is possible to explore combination therapies that exploit the disrupted blood–tumor barriers.

INTRODUCTION

Chimeric antigen receptor (CAR)-based T-cell therapies have failed to make noticeable clinical progress in solid tumor treatment.^{1 2} A meta-analysis of clinical studies identified no clinical study with meaningful therapeutic efficacies against solid tumors using CAR T technologies.^{3 4} Complex challenges encountered by CAR T-cell therapies in solid tumors include the presence of targets in normal tissues, leading to on-target off-tumor toxicities and safety issues,^{5–7} inhibition of CAR T cells by the tumor microenvironment (TME) on entering tumor tissues,^{8 9} and poor persistence of infused CAR T cells originating

from in vitro-expanded T cells.¹⁰ To overcome these challenges, cell engineering techniques must effectively navigate through tumor barriers, surmount hindrances posed by the tumor stromal extracellular matrix, overcome immune-suppressive cells and factors, and counteract T-cell exhaustion and senescence.⁸ In addition, the lack of a sustained activation state of infused CAR T cells against solid tumors has prompted engineering efforts toward cytokine-fortified CAR T cells to generate resistance against a suppressive TME.⁸

Recently, claudin 18.2-targeting CAR T cells achieved transient reductions in tumor sizes when treating digestive system cancers but led to no durable remissions, in contrast to treating hematological tumors using CAR T cells.¹¹ The durable proliferation of CAR T cells by engineered IL-2 signaling pathways has been observed,^{12–13} creating ‘armored’ CAR T cells.^{9–14} As an alternative approach, the combined use of checkpoint inhibitors such as PD-1 antagonists and CAR T cells has controlled and inhibited tumor growth in animal studies.^{15–16} Stimulation of the in vivo proliferation of CAR T cells has been achieved by antigen delivery to antigen-presenting cells (APCs) in lymphoid tissue¹⁷ or by an RNA vaccine that transfected APCs in vivo,¹⁸ again aiming at increasing the durability of functional CAR T cells.

To minimize the impact of the suppressive TME, we focused on targeting the tumor vasculature using CAR T cells. Two fibronectin splicing variants, containing extra domain B (EDB) or EDA, appear to be expressed on endothelial cells and may be involved in forming neovasculature during angiogenesis.¹⁹ Earlier studies showed that EDB-fibronectin is exclusively expressed during embryo development or tumor angiogenesis.^{20–22} EDB-fibronectin has been explored as a potential drug target for treating solid tumors.²³ Recently, second-generation CAR T cells targeting EDB were shown to possess low inhibitory activities toward the growth of small tumors in vivo.^{24–25} The reasons for the underperformance of second-generation EDB CAR T cells were unclear. However, it was probably because EDB-fibronectin exists in multiple forms that are mostly interlocked into the ECM of cancer cells, endothelial cells, or cancer-associated fibroblasts or are embedded in fibrillar structures in tumor tissues.^{21–22–26–29} It also needs to be clarified whether the absence of membrane fluidity for fibronectins caused the suboptimal activation of EDB-targeting CAR T cells.

Chimeric receptors have been integrated into T cell receptors (TCRs) as a viable alternative to the single chain format seen in the second G CAR. This incorporation allows for the redirection of TCRs toward specific targets of interest. Initially, a single-chain variable fragment (scFv) fused to CD3 ζ was found to be incorporated into the TCR, and the resulting receptors demonstrated superior antigen responses.^{30–31} In their work, Baeuerle *et al* expanded on TCR fusions by designing protein fusions with other TCR subunits, and the resulting chimeric TCRs were referred to as TRuC.³² In the current study, we provide evidence that an EDB-recognizing scFv fused to

the TCR structure with an added costimulatory molecule can inhibit neovasculature formation in tumor tissues, assemble into superior immune synapse structures, and efficiently suppress tumor growth in vivo.

MATERIALS AND METHODS

Cell lines

The human cancer cell lines U87MG, A549, and Jurkat E6.1 were purchased from the Cell Bank of the Chinese Academy of Sciences (Shanghai, China). The Raji cell line was a gift from the Center for New Drug Safety Evaluation and Research, China Pharmaceutical University. The presence of EDB antigen was confirmed by flow cytometry or Western blot analysis using an EDB-specific L19 antibody and qPCR analysis. The 293F cell line for lentivirus packaging was a gift from Satuit Therapeutics, Woburn, Massachusetts, USA. Jurkat-CD3 ϵ , CD3 ζ , LAT, or LCK KO cells were derived from Jurkat E6.1 cells by knocking out CD3 ϵ with the CRISPR-Cas9 system [guide RNA (gRNA) sequences: CD3 ϵ _CTGGATTACCTCTTGCCCTC, CD3 ζ _TTTCACCGCGGCCATCCTGC, LCK_GACCCACTGGT-TACCTACGA, LAT_ACGACAGCACATCCTCAGAT]. U87MGEDB KO cells were derived from U87MG cells by knocking out EDB with the CRISPR-Cas9 system [guide RNA (gRNA) sequences: EDB_GCTCTTCGAGGCTCCC GTGGAGG].

Construction of chimeric receptors and preparation of CAR⁺ cells

L19-scFv, an anti-EDB-FN-specific scFv, was derived from the humanized EDB antibody L19³³ (GenBank accession: AJ006113.2). The 28z and BBz CARs contained extracellular domains of the CD8 α hinge and transmembrane domains, followed by the intracellular domains of CD28 or 4-1BB and CD3 ζ . EFL, EFL28, and EFL137 are chimeric receptors containing L19-scFv fused to full-length CD3 ϵ . The EFL28 or EFL137 incorporated the CD28 or 4-1BB intracellular signaling domains at the C-terminus of CD3 ϵ , respectively. Isolation, transduction of primary human T cells, expansion of rTCR-CAR T cells, and preparation of lentiviral vectors were carried out as previously described.³⁴

Analysis and purification of CAR⁺ T cells

To analyze the CAR⁺ T cells, 10⁶ transduced T cells were incubated with 8 μ g/mL reconstituted biotin-labeled polyclonal goat anti-human-F(ab)₂ antibodies (109-066-097, Jackson ImmunoResearch) in FACS buffer (PBS plus 0.4% FBS) for 25 min at 4°C. Cells were washed with FACS buffer and incubated with phycoerythrin (R-phycoerythrin streptavidin, 016-110-084, Jackson ImmunoResearch) in FACS buffer for 20 min on ice in the dark. Cells were washed three times with an ice-cold FACS buffer and analyzed on an ACEA Novocyte Flow Cytometer. For flow-cytometric analysis, the following antibodies were used: Alexa Fluor 488 anti-human CD279 (PD-1) antibody (329936, BioLegend), APC anti-human

CD223 (LAG-3) antibody (369212, BioLegend), PerCP/Cyanine5.5 anti-human CD366 (Tim-3) antibody (345016, BioLegend), FITC anti-human CD25 antibody (302604, BioLegend), and APC anti-human CD69 antibody (310910, BioLegend). The CellTrace Far Red Cell Proliferation Kit (34564, Thermo Fisher Scientific) and FITC anti-human CD107a (LAMP-1) antibody (328606, Thermo Fisher Scientific) were also used.

To purify the CAR⁺ T cells, biotin goat anti-human-F(ab)₂ antibody-coated T cells, as described above, were incubated for 15 min with streptavidin nanobeads (480016, BioLegend) on ice, and the CAR⁺ T cells were isolated by magnetic separation using MojoSort Buffer (480017, BioLegend).

Detection of CAR⁺ T cells by qPCR using the MGB probe

Total DNA extraction and qPCR were performed using MiniBEST Whole Blood Genomic DNA (9781, Takara) and qPCR kits (RR390, Takara). CAR F-primer: 5'-CACCGATTTTACCCTGAC-3', and R-primer: 5'-GCCAAAGGTAGGAGGAATA-3'; MGB-probe: 5'-6-VIC-AAGACTTCGCCGTGTATTA-MGB-3'.

Cytotoxicity assays and in vitro cytokine release assay

To assay the cytotoxicity of CAR T cells, target cells were mixed with transduced T cells in various effector-to-target ratios in a 96-well U-bottom plate for 24 hours, and cell lysis was detected by an LDH detection kit (G1780, Promega). Cytokine analysis was carried out using IFN- γ ELISA (1110002, Dakewe) and TNF- α ELISA (1117202, Dakewe).

Immune synapse imaging

28z-EGFP, EFL-EGFP, and EFL28-EGFP contain EGFP fused to CARs and were constructed by homologous recombination, and CAR T cells were prepared by lentiviral transduction. A 1 mg of biotinylated EDB-FN protein was incubated with 20 mg of SA beads (480016, BioLegend) at 4°C for 8 hours. The magnetic beads were washed with DPBS. 5×10^4 28z CAR T, EFL, or EFL28 rTCR-CAR T cells were incubated with 100 μ g EDB-FN beads in a 96-well U-bottom plate for 10 min, and the cells bound to the magnetic beads were sorted. Cells were spread on glass slides, fixed with paraformaldehyde for 20 min, and observed under a laser confocal microscope (LSM 700, ZEISS) after adding DAPI.

Coimmunoprecipitation, phosphorylation assay, and Western blot

For coimmunoprecipitation (co-IP) and Western blot, we used anti-TCR α (sc-515719, Santa Cruz Biotechnology), anti-TCR β (9485, Cell Signaling Technology), anti-CD3 ζ (A11157, ABclonal), anti-CD3 γ (A4085, ABclonal), anti-CD3 δ (A9770, ABclonal), anti-CD3 ϵ (sc-20047, Santa Cruz Biotechnology), anti-pCD3 ζ -Y142 (ab68235, Abcam), anti-LCK (2657, Cell Signaling Technology), anti-pLCK-Y394 (AP0182, ABclonal), anti-PLC γ (2822, Cell Signaling Technology), anti-PLC γ (2821, Cell Signaling Technology), anti-NFATc1

(5861, Cell Signaling Technology), anti-NF- κ B p65 (6956, Cell Signaling Technology), anti-ZAP70 (3165, Cell Signaling Technology), anti-pZap70 (2701, Cell Signaling Technology), peroxidase-conjugated goat anti-rabbit IgG (33 101ES60, Yeasen), peroxidase AffiniPure goat anti-mouse IgG (33 201ES60, Yeasen), streptavidin magnetic beads (P2151, Beyotime Biotechnology), NP-40 lysis buffer (P0013F, Beyotime Biotechnology), Nuclear and Cytoplasmic Protein Extraction Kit (20 126ES50, Yeasen), protease inhibitor cocktail (20 124ES03, Yeasen), phosphatase inhibitor cocktail (20 109ES05, Yeasen), and a co-IP kit (26149, Thermo Fisher Scientific).

For immunoprecipitation analysis, 10⁷ CAR expression-positive cells were lysed in 200 μ L NP-40 lysis buffer containing protease and phosphatase inhibitor cocktail for 60 min at 4°C, followed by 10 min of centrifugation to remove insoluble material. For the anti-TCR β co-IP, 100 μ L lysate was incubated with 2 μ L anti-TCR β antibody and 5 μ L protein G beads for 1 hour at 25°C. For the anti-human-F(ab)₂ co-IP, 100 μ L lysate was incubated with 5 μ L anti-TCR β antibody and 5 μ L streptavidin magnetic beads for 1 hour at 25°C.

Transduced T cells were serum-starved overnight for phosphorylation analysis to reduce background phosphorylation. For Western blot, cells were collected in an NP-40 lysis buffer containing a protease and phosphatase inhibitor cocktail for 30 min at 4°C prior to anti-phosphorylation Western blot analysis.

Antitumor efficacy in NCG mouse tumor models

Female NCG (NOD/ShiLtJGpt-Prkdc^{em26Cd52}Il2rg^{em26Cd22}/Gpt) mice aged 6–8 weeks were obtained from GemPharmatech (Jiangsu, China) and housed in SPF conditions at China Pharmaceutical University. Tumor models were established by subcutaneous injection of cancer cells and mice were randomly assigned to treatment or control groups. Mice were euthanized once humane endpoints were reached, which included tumors larger than 17 mm or a loss of body weight greater than 15%. To establish A549 or U87MG tumor models, approximately 1 million cancer cells were injected subcutaneously on the dorsal-lateral side, respectively, and tumor growth was monitored every 3–4 days. Transduced CAR T cells were infused by tail vein injection. To test dose responses, 1, 5, or 25 million transduced EDB CAR T cells were infused by tail vein injection into the mice. For U87MG or U87MG^{EDB KO} large tumor models, 1 million tumor cells were injected subcutaneously to establish tumors on the dorsolateral side. Once the tumors were palpable and the tumor sizes measured approximately 100 mm³, mice were randomly grouped (5/group). Two doses of 10 million transduced CAR T cells were each infused by tail vein injection into the mice on the 1st and the 14th day, respectively. Immunohistochemistry (IHC) was performed on tumors removed

from the models to detect the infiltration of CAR T cells into tumor tissue.

IHC analysis

Lung adenocarcinoma tissues were obtained from the Shandong Academy of Medical Sciences. Eighty-one sarcoma samples in a K105Sf01 microarray (K105Sf01) were purchased from Bioaitech, and 120 normal human tissues in a microarray (HOrgN120PT01) were purchased from Outdo Biotech. These samples were immunostained by using the anti-EDB antibody L19. Infiltrating T cells were detected on tumor tissues extracted 14 days after CAR T cell infusion. IHC for infiltrating T cells was performed as previously described³⁴ using an anti-CD3 antibody (ab16669, Abcam). Blood vessels in the tumor tissues were detected using an anti-CD31 antibody (A19014, ABclonal).

Test of CAR T-cell toxicity in mice

In the *in vivo* toxicity evaluation experiment of CAR T cells, 10 NCG mice aged 8 weeks were randomly divided into the T-cell group (n=3) and EFL28 rTCR-CAR T cell group (n=3). One dose of 1×10^7 T cells or 1×10^7 EFL28 rTCR-CAR T cells was intravenously injected via the tail vein in 200 μ L of physiological saline. All mice were sacrificed on day 14 following T-cell infusion. Different tissues were harvested, formalin-fixed, paraffin-embedded, and stained with H&E.

Isolation of endothelial cells from fresh tissues

U87MG^{EDB KO} tumor model mice were sacrificed, and tumor and kidney tissues were extracted. The tumor and kidney tissue were digested into cell suspensions by the KeyGEN tissue dissociation Kit (KGA829, KeyGEN). Mouse CD31⁺ endothelial cells were isolated from cell suspensions derived from U87MG^{EDB KO} tumors or kidneys using CD31 MicroBeads (130-097-418, Miltenyi).

NGS RNAseq

Library preparation and Illumina sequencing were conducted at GENEWIZ (Suzhou, China) using 1 μ g of total RNA from various cells. HTSeq (V.0.6.1) was used to estimate gene and isoform expression levels from the paired-end-cleaned data. Differential expression analysis was performed using the DESeq2 Bioconductor package based on a negative binomial distribution model. The estimates of the dispersion and logarithmic fold changes of gene expression incorporated data-driven prior distributions. The significance score *P*_{adj} for gene expression differentials was set at <0.05.

Statistical analysis

Two-tailed non-parametric t-tests for unpaired data were used to analyze differences between two groups. One-way analysis of variance (ANOVA) or two-way ANOVA was used to compare multiple groups. *In vivo* survival data were plotted using a Kaplan-Meier curve, and differences between groups were determined using the log-rank test.

RESULTS

Expression profile of EDB in tumor and normal tissues

Most solid tumors express EDB-fibronectin, which can be detected on both tumor cells and the endothelial cells of the tumor neovasculature.^{20–22} Through IHC analysis, we investigated the expression of EDB in lung cancer tissues and observed a correlation between the EDB-fibronectin expression level and the progression of non-small cell lung cancer (online supplemental figure S1A,B and table S1). This finding is consistent with similar findings for breast cancer or B-cell lymphomas.^{21 35 36} In addition, EDB-fibronectin was significantly enriched in the endothelial layers of tumor vessels in sarcoma samples (online supplemental figure S1C,D). However, it was absent in 36 normal human tissues (online supplemental figure S1E), suggesting that EDB-fibronectin may be a more suitable cell therapy target in treating sarcoma cancers since redirected CAR T cells may achieve effectiveness without penetrating the endothelium layer.

GENERATION OF rTCR-CAR T CELLS

Previously, EDB-targeting second-generation CAR T cells were inadequate *in vivo* against solid tumors.^{24 25 34} To explore alternative approaches targeting the EDB-fibronectin, we fused the scFv from the EDB-specific L19³³ to the N-terminus of the CD3 ϵ subunit of TCR and attached various intracellular domains of costimulatory molecules to the C-terminus of the CD3 ϵ (figure 1A). The scFv and the costimulatory domains were expected to be incorporated into the TCR complex, and the resulting complexes were termed as redirected TCR-CAR, or rTCR-CAR (designated as EFL, EFL28, and EFL137 in figure 1A). In comparison, we made second-generation CARs using the same scFv and incorporating either a 4-1BB or CD28 intracellular domain, as shown in figure 1A (designated as 28z and BBz). Cell surface expression of second-generation CARs or rTCR-CAR was readily detected in transduced primary human T cells from six different donors, as exemplified in online supplemental figure S2A for one donor. Transduction efficiencies were not biased toward either CD4 or CD8 subset (online supplemental figure S2B). To verify the incorporation of the CD3 ϵ chimeras into the rTCR-CAR complex, we purified rTCR-CAR-transduced Jurkat cells (online supplemental figure S2C), used anti-scFv or anti-TCR β antibodies to immunoprecipitate (IP) TCR complexes, and analyzed the IP by Western Blot (figure 1B,C). Along with the scFv-containing CD3 ϵ fusions, CD3 ζ , CD3 δ , CD3 γ , TCR α , and TCR β proteins were precipitated with the anti-scFv antibodies (figure 1B), suggesting that the rTCR-CAR complexes incorporated the chimeric CD3 ϵ . The expression levels of the native CD3 ϵ were comparable to those of the chimeric CD3 ϵ in whole cell lysates (figure 1D). However, when subjected to anti-TGF β precipitation, a greater amount of chimeric CD3 ϵ was pulled down, indicating a higher affinity or binding preference for the chimeric form in this context (figure 1C). Further,

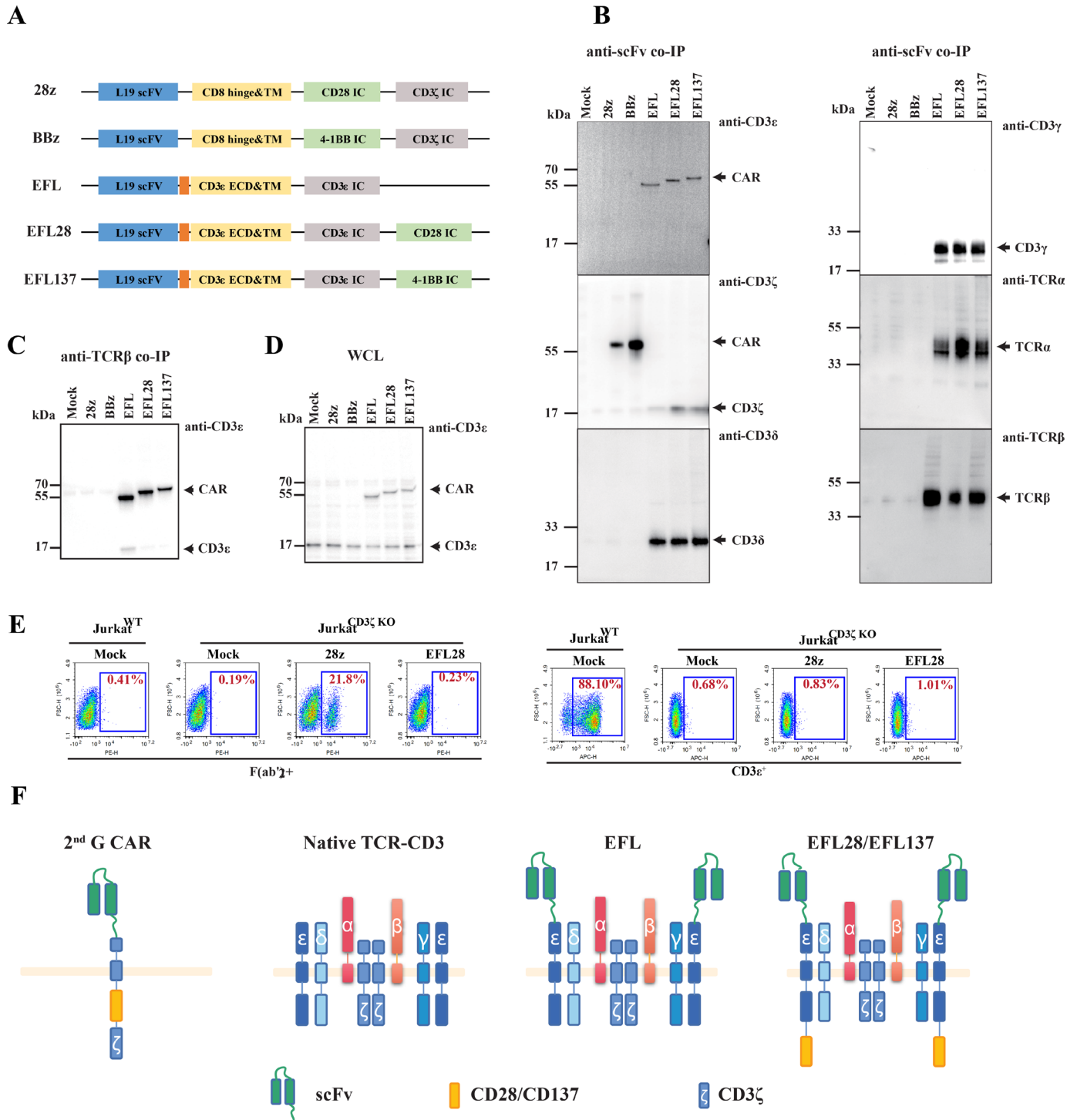


Figure 1 Cell surface expression of EDB-targeting chimeric receptors and incorporation into the TCR complex. (A) Schematic representation of chimeric antigen receptors containing L19 scFv. BBz and 28z: second-generation CARs; EFL, EFL28, EFL137: rTCR-CARs. (B) Immunoprecipitation and Western blot analysis of second-generation CARs or rTCR-CAR complexes using transduced and purified EDB CAR⁺ Jurkat T cells. TCR α , TCR β , CD3 ζ , CD3 γ , and CD3 δ are associated with rTCR-CARs, but not second-generation CARs. (C) rTCR-CARs but not second-generation CARs can be precipitated by using anti-TCR β antibodies. (D) Whole-cell lysate Western blotting using anti-CD3 ϵ antibody; (E) CD3 ζ KO Jurkat T cells on transduction expressed second-generation CAR but not rTCR-CAR on the surface of cell membranes. (F) Schematics of the predicted rTCR-CAR structures and their differences from second-generation CARs. co-IP; coimmunoprecipitation; EDB, extra domain B; scFv, single-chain variable fragment.

precipitation with anti-scFv resulted in a lower amount of CD3 ζ and TCR α being pulled down in the EFL rTCR-CAR construct (figure 1D), compared with the EFL28 and

EFL137 rTCR-CAR constructs. Thus, the chimeric CD3 ϵ with fusions at both N-termini and C-termini exhibited

the highest levels of incorporation into the rTCR-CAR complex. Additionally, the presence of chimeric CD3 ϵ made it less likely for the native CD3 ϵ to be incorporated into the complex. Although the exact mechanism behind the favored incorporation of the chimeric CD3 ϵ with a costimulatory domain remains unclear, it is unlikely to be attributed to its overexpression. The analysis of whole cell lysates revealed that the expression levels of the chimeric CD3 ϵ were similar (figure 1D).

The expression of rTCR-CARs was absent in CD3 ζ -knockout Jurkat cells (figure 1E and online supplemental figure S3A,B). It has been shown previously that TCR assembly requires the formation of the CD3 ζ dimer.^{37,38} Our data indicated that the rTCR-CAR assembly pathway is similar to that for TCR. The proposed structures representing rTCR-CAR in this study are depicted schematically in figure 1F.

In vitro cytotoxicity and superior formation of immune synapses by rTCR-CAR T cells

Fibronectins are typically embedded in the extracellular matrix. EDB-fibronectin was readily detected by

flow cytometry (online supplemental figure S4A). EDB-targeting second-generation or rTCR-CAR T cells demonstrated cytotoxicity toward EDB⁺ U87MG, A549, and Raji cells (figure 2A–C) but not the EDB-knockout U87MG cells (online supplemental figure S4B–D). No discernable differences in cytotoxicity were found between the second-generation 28z and rTCR-CAR EFL28 T cells (figure 2A–C). Irrespective of whether the EDB CAR was a second-generation CAR or rTCR-CAR format, the addition of the CD28 intracellular domain significantly amplified the cytotoxicity, higher than attaching the 4-1BB intracellular domain (figure 2A–C). EDB⁺ U87MG cells upregulated the T-cell activation markers CD69 and CD25 on the CAR T cells (figure 2D,E), suggesting that EDB fibronectin activated the second-generation or rTCR-CAR T cells despite being an immobile antigen. The degranulation markers CD107a and granzyme B were increased, suggesting that the target cells were perforated and became apoptotic (figure 2F,G). In vitro, the rTCR-CAR with CD28 intracellular domain exhibited more CD69, CD25, and granzyme B markers than the

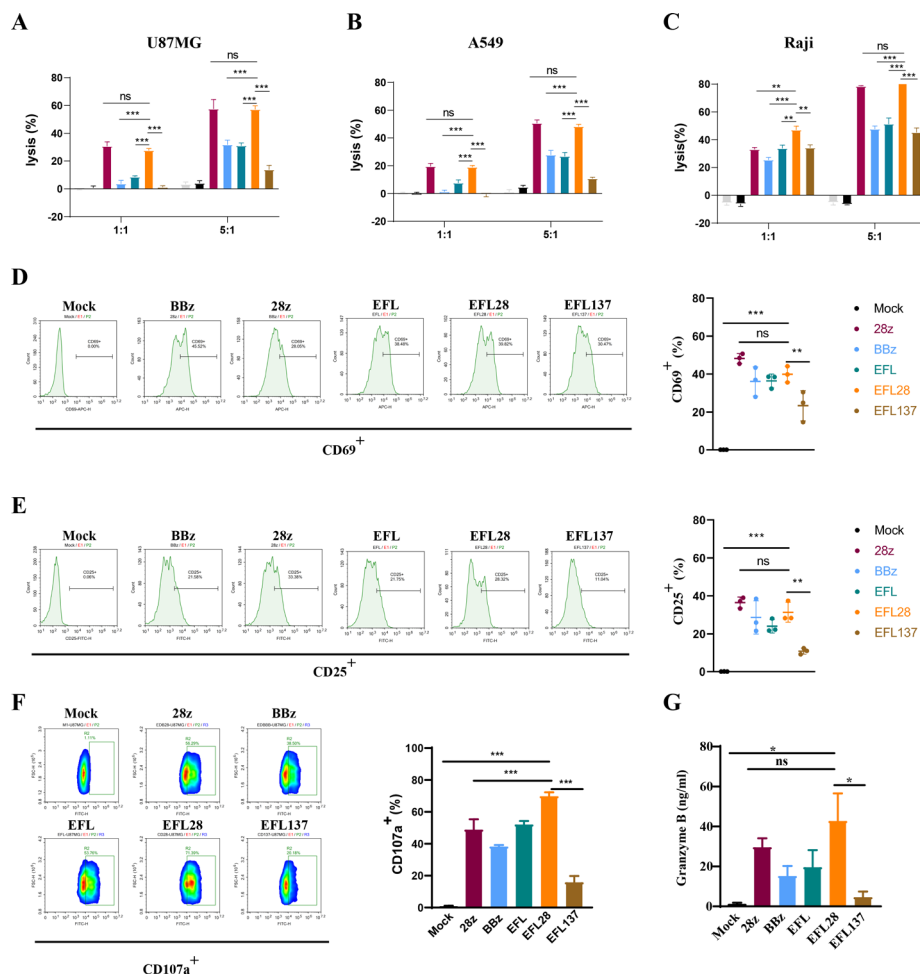


Figure 2 Cytotoxic activities of EDB-targeting second-generation CAR or rTCR-CAR T cells in vitro. (A–C) CAR T cells are cytotoxic to EDB-positive U87MG, A549, and Raji cell lines, $n=3$. (D–G) T-cell activation markers CD69, CD25, CD107a, and Granzyme B were induced by incubation with U87MG and detected by flow cytometry or ELISA. Quantitation of CD69, CD25, and CD107a upregulation in transduced T cells from three individuals. Student's two-tailed unpaired t-test was used to determine the statistical significance between the indicated groups. * $p<0.05$, ** $p<0.01$, *** $p<0.001$. EDB, extra domain B.

rTCR-CAR with 4-1BB intracellular domain, consistent with the observed differences in cytotoxicity.

Under the stimulation by EDB antigen conjugated to magnetic beads, EFL28 rTCR-CAR T cells formed visibly more discrete receptor clusters with the highest intensities, suggesting increased sequestration of the EFL28 rTCR-CAR (online supplemental figure S5). In contrast, the same antigen stimulation led to the formation of only diffuse receptor structures on the surface of second-generation 28z EDB CAR T cells (online supplemental figure S5A-D). TCR-CD28 microclusters were reported to accumulate in mature immune synapses, where CD28 assembles with signaling kinases and generates sustained T-cell signaling.³⁹ Similarly, using a second-generation CAR as a model, others found that sequestered second-generation CAR on the cell surface lacked authentic TCR immune synapses.⁴⁰ Immune synapse quality is directly correlated with the effectiveness of CAR T cells *in vivo*.⁴¹ Here, we observed more intense receptor clusters of the rTCR-CAR, suggesting that stimulation of rTCR-CAR led to superior immune synapses compared with that formed by the second-generation CAR. It is intriguing to explore whether this discovery can be extrapolated to other antigens.

Superior *in vivo* efficacy of EFL28 rTCR-CAR T cells

In vivo function of rTCR-CAR T cells was evaluated using the xenograft model. In small A549 or U87MG tumors with roughly 50 mm³ volumes, T cells demonstrated notably the most tumor growth suppression, whereas the second-generation CAR T cells showed negligible inhibition of the tumor growth in the *in vivo* experiment (figure 3A–D). The inhibition of the U87MG tumor by EFL28 rTCR-CAR cells was dose-dependent (online supplemental figure S6A–L). Complete eradication of tumors was observed for 3/5 of the mice in the 2.5×10⁷ EFL28 rTCR-CAR T group (online supplemental figure S6J–L). The EFL rTCR-CAR lacked any intracellular domains of a costimulatory molecule, resulting in only mild inhibition with no complete regression (figure 3A–D, online supplemental figure S6). This observation suggests that costimulatory signal such as the CD28 intracellular domain is crucial for the *in vivo* performance of rTCR-CAR.

It has been suggested that tumor sizes greater than 100 mm³ in animal models are considered established and immunosuppressive, and most human malignancies exceed this critical size limit with significant margins.⁴² To assess the effectiveness of the rTCR-CAR T cells under immune suppressive conditions, we examined large U87MG tumors ranging from 100 to 150 mm³ in volume. The EFL28 rTCR-CAR T cells were found to significantly inhibit the growth of large tumors, whereas the second-generation CAR was barely adequate (figure 3E–H). This indicates that rTCR-CAR T cells targeting EDB can be functional in presence of the suppressive TME.

EFL28 rTCR-CAR T cells inhibit tumor growth by disrupting the tumor neovasculature

To understand how the EFL28 rTCR-CAR T cells inhibited the growth of large tumors, we examined the possibility that the tumor neovasculature was used by the CAR T cells as a target in the large tumor models. As previously stated, EDB-fibronectin was found to be enriched in the blood vessels of tumors (online supplemental figure S1C). By IHC, we showed that the tumor vessel densities in the EFL28 rTCR-CAR group were significantly lower than those in the 28z CAR or T-cell groups (figure 4A,B). To validate that the inhibition of the tumor neovascularization by the EDB CAR-T cells retarded tumor progression, we established U87MG^{EDB KO} tumors. EFL28 rTCR-CAR T cells also had an inhibitory effect on U87MG^{EDB KO} tumors and prolonged mouse survival (figure 4C,D), in contrast to earlier findings using second-generation CAR.²⁴ Thus, our data strongly suggest that tumor growth inhibition in xenograft models is partly mediated by killing EDB-positive endothelial cells in the neovasculature. To further substantiate this finding, vascular endothelial cells were extracted from the kidneys and tumors of U87MG^{EDB KO} tumor-bearing mice, and we observed that EDB-positive tumor endothelial cells were killed by EDB rTCR-CAR T cells, but not the renal tissue-derived and EDB-negative endothelial cells (figure 4E,F). Thus, our results indicate that targeting neovasculature in a therapeutic approach could potentially overcome the hindrances posed by the TME to T cell therapies. Moreover, the EDB rTCR-CAR T cells eliminated EDB-positive endothelial cells in tumor neovasculature, a feature that makes them suitable for treating tumors composed of EDB-negative cancer cells.

EFL28 rTCR-CAR T cells are not toxic and persist better *in vivo*

We injected the T cells via the tail vein and monitored their distribution to understand how the rTCR-CAR T cells identified the EDB antigen and whether there was any accumulation within the xenograft tumors. The amino acid sequences of mouse and human EDB are nearly identical, and the L19 scFv can specifically recognize human and mouse EDB.^{33 43} To evaluate the distribution and safety of EFL28 rTCR-CAR T cells in mice, EFL28 rTCR-CAR T or control T cells were labeled with a fluorescence probe and infused into mice bearing large tumors. Tumor tissues showed a higher concentration of EFL28 rTCR-CAR T cells than untransduced T cells (online supplemental figure S7A). The distribution of EFL28 rTCR-CAR T cells in the normal tissues was similar to that of T cells (Online supplemental figure S7A). EFL28 rTCR-CAR T cells had no discernable toxicity to normal tissues or organs of the mice (online supplemental figure S7B), suggesting that EFL28 rTCR-CAR T cells did not induce on-target off-tumor toxicities in the *in vivo* mouse models. Immunohistochemical analysis showed that 28z, EFL, and EFL28 CAR T cells all infiltrative tumor tissue, although the activation status of the infiltrated CAR T cells could not be verified (figure 5A,B). Detection of the CAR gene copy number in the peripheral blood of mice

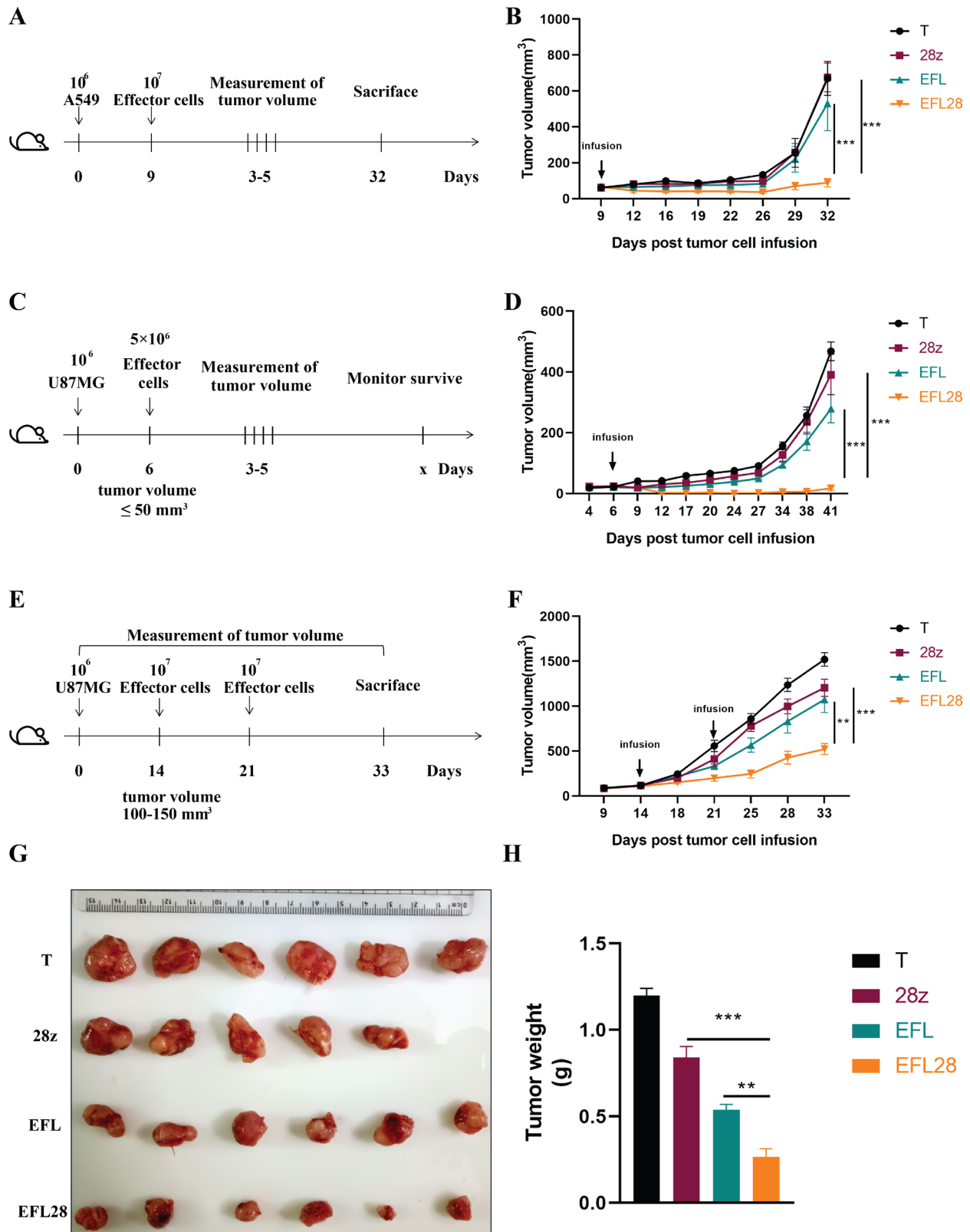


Figure 3 Anti-EDB rTCR-CAR T cells demonstrated the most tumor growth inhibition in NCG mice. (A) Schematics for the A549 tumor in vivo testing. (B) Ten million effector cells were intravenously administered, $n=5$. (C) Schematics for the U87MG tumor (tumor volumes $<50\text{ mm}^3$) in vivo testing. (D) Ten million effector cells were intravenously administered, $n=5$. (E, F) NCG mice were subcutaneously inoculated with 10^6 U87MG cells on day 0. Two doses of 10^7 EDB-targeted CAR T cells or T cells were intravenously administered on days 14 and 21. Tumor growth is presented as the mean tumor volume and SEM. (G, H) On day 33 after tumor cell inoculation, the mice were euthanized. Tumor weight was measured, and statistical significance for the difference was analyzed by two-way analysis of variance with Bonferroni post hoc test. Survival was plotted using a Kaplan-Meier curve, and statistically significant differences were analyzed using the log-rank test, $**p<0.01$, $***p<0.001$.

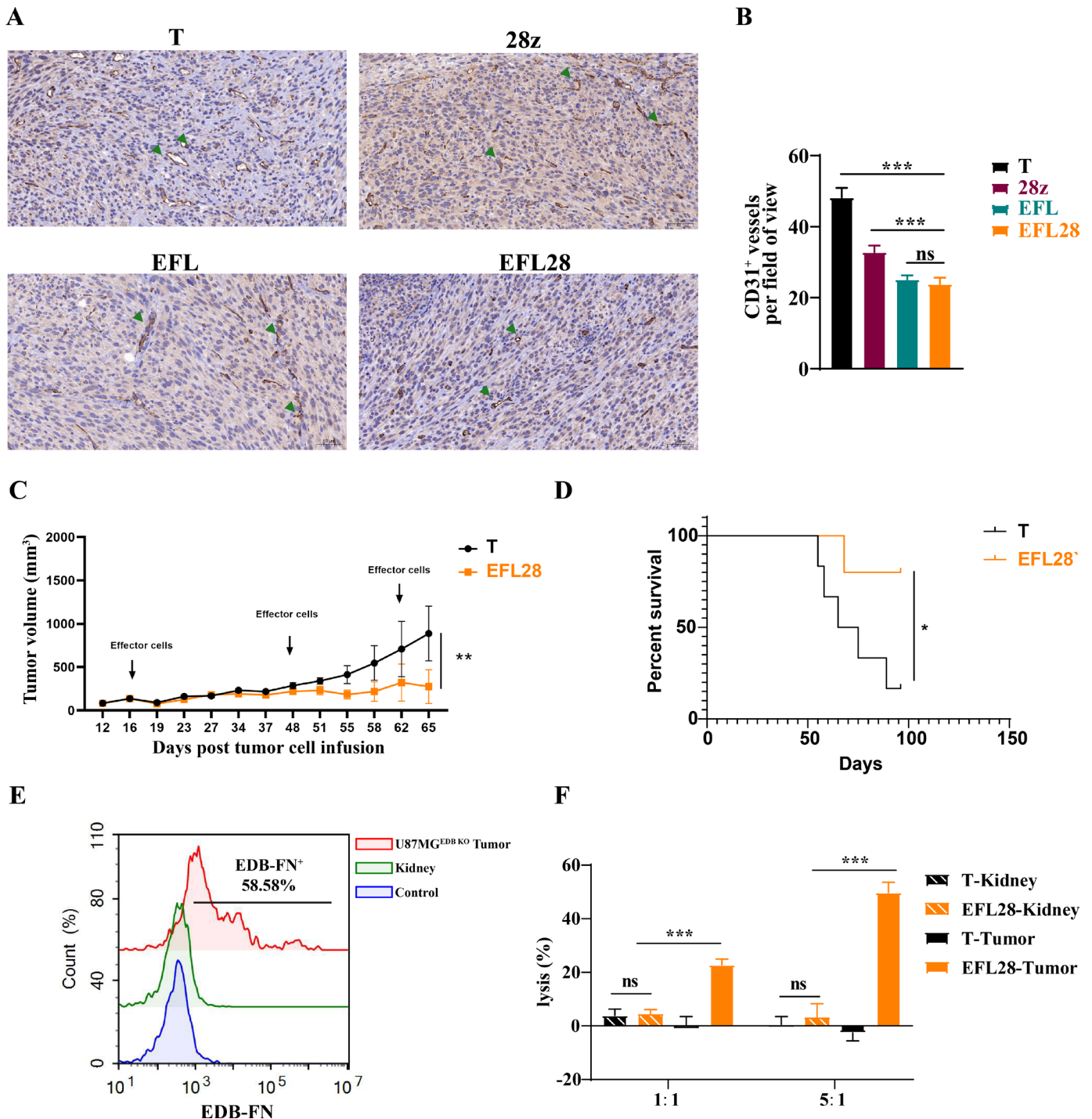


Figure 4 EFL28 rTCR-CAR T cells reduce tumor blood vessels. (A) 10^7 CAR T cells or T cells were injected into the tail vein of U87MG tumor-bearing mice, tumor tissues were collected on the 14th day, and tumor-associated vascular endothelial cells were detected by immunohistochemistry using an anti-CD31 antibody. (B) Quantitation of CD31⁺ vessels. Statistical significance was calculated by one-way analysis of variance (ANOVA) with Bonferroni post hoc test, $n=5$, $***p<0.001$. (C) Tumor growth of different groups. Statistical significance was calculated by two-way ANOVA; mice treated with T cells, $n=6$; mice treated with EFL28 rTCR-CAR T cells, $n=5$. $**p<0.01$ (D) Survival plot using a Kaplan-Meier curve. Statistically significant differences were determined using the log-rank test, $*p<0.05$. (E) CD31-positive cells were isolated from the kidneys and tumors of U87MG^{E₂B}^{KO} tumor-bearing mice. EDB expression in vascular endothelial cells of the kidney or U87MG^{E₂B}^{KO} tumors was analyzed by flow cytometry using the L19 antibody. (F) CAR T cells were cytotoxic to EDB-positive cells of tumor origin but not to endothelial cells from the kidney. Statistical significance was calculated by one-way ANOVA with Bonferroni post hoc test, $n=3$, $***p<0.001$. EDB, extra domain B.

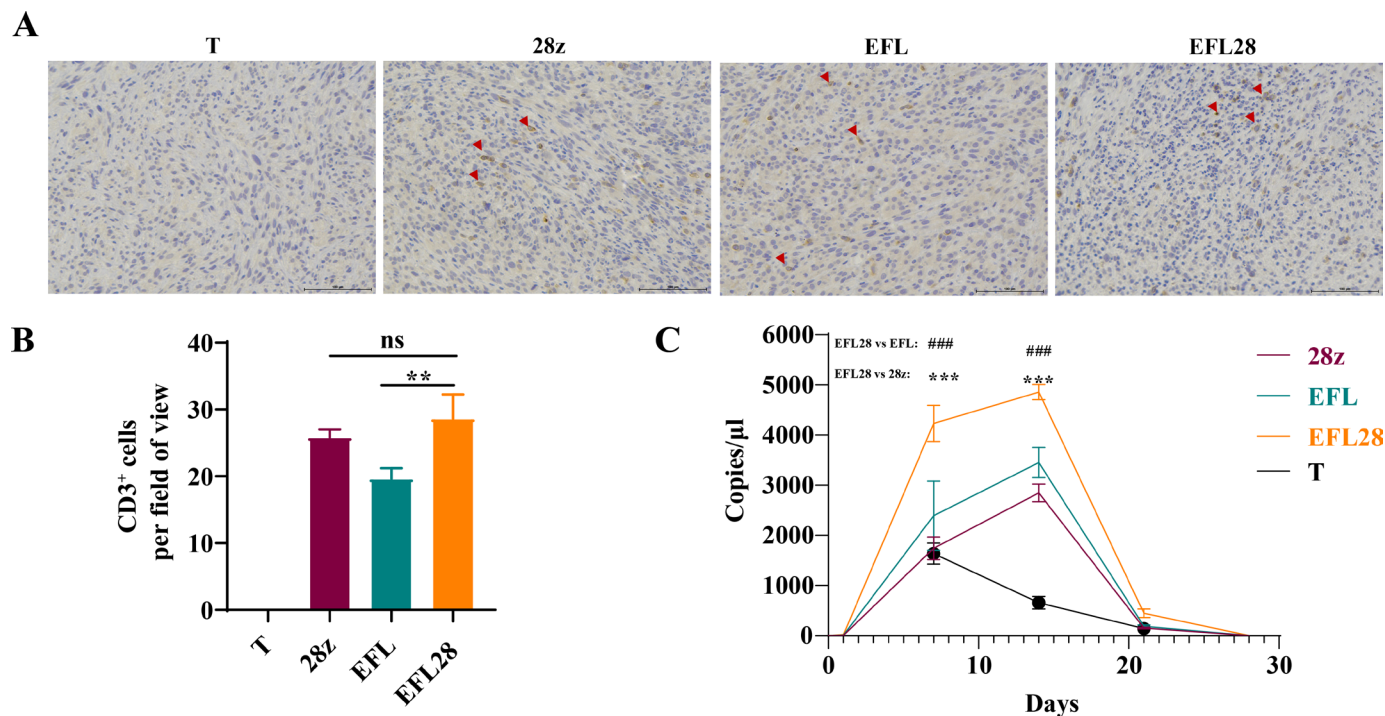


Figure 5 Infiltration and persistence of EFL28 rTCR-CAR T cells in large tumors in vivo. (A) 10^7 CAR T cells or T cells were injected into the tail vein of U87MG tumor-bearing mice, and tumor tissues were collected on the 14th day. Infiltrating T cells were detected by immunohistochemistry using an anti-CD3 antibody. Red arrow heads denote CD3⁺ CAR T cells (B) Quantification of CD3⁺ cells in tumor tissues. Statistical significance was calculated by one-way analysis of variance (ANOVA) with Bonferroni post hoc test, $n=5$, $**p<0.01$. (C) 10^7 CAR T cells were injected into the tail vein of U87MG tumor-bearing mice, and peripheral blood was collected on days 0, 1, 7, 14, 21, and 28 to extract DNA. The copy number of the CAR gene or T cells in peripheral blood was detected by qPCR, $n=5$. Statistical significance was calculated by one-way ANOVA with Bonferroni posttest, $***p<0.001$; $###p<0.001$.

revealed that EFL28 rTCR-CAR T cells had the highest proliferation ability in mice (figure 5C), which correlated with their superior efficacy in vivo (figure 3).

EFL28 rTCR-CAR mediated higher phosphorylation of ERK or ZAP70 than the second-generation CAR or rTCR-CAR without costimulatory signals (figure 6A and online supplemental figure S8A-F). Phosphorylation of NFκB p65 was also the highest with the EFL28 rTCR-CAR construct, while phosphorylation of NFATc1 was higher with the 28z CAR construct (figure 6B). Phosphorylation of ERK and CD3ζ142, downstream of EFL28 rTCR-CAR, was dependent on the TCR signaling proteins LCK and LAT, as the phosphorylation in the LCK-knockout or LAT-knockout strains (online supplemental figure S3C-F) was abrogated entirely (figure 6C,D). Taken together, though fully embedded without lateral membrane fluidity in the extracellular matrices, the EDB-fibronectin functioned as a common T-cell antigen and stimulated T cells through traditional TCR signaling pathways. To rule out that indigenous CD3ε was required for chimeric TCR signaling, we used CRISPR editing to delete the CD3ε gene from Jurkat cells (online supplemental figure S9A,B). The phosphorylation driven by EFL28 rTCR-CAR signaling was independent of CD3ε knockout, suggesting that rTCR-CAR signaling did not require native CD3ε and that the signaling function through chimeric CD3ε was sufficient (online supplemental figure S9C).

rTCR-CAR T cells are activated through the TCR signaling pathway

rTCR-CAR-modified T cells show T-cell-like activation

We noticed that without antigen stimulation, the CD69⁺ ratio of the EFL28 rTCR-CAR T cells was lower than that of the 28z CAR T cells (figure 7A), indicating a higher residual activation state or antigen-independent tonic signaling in the second-generation, 28z CAR T cells. The tonic signaling in 28z CAR T cells was also confirmed by the higher expression levels of IFN-γ and IL-2 in the quiescent state (figure 7B,C). Transcriptome sequencing of unstimulated cells showed that the expression levels of genes related to T-cell activation were lower in EFL28 rTCR-CAR T cells than in the second-generation, 28z CAR T cells and were more comparable to those in T cells (online supplemental figure S10A,B). Phosphorylation Western blot analysis also confirmed that the CD3ζ142 amino acid residue in CAR or endogenous CD3ζ had higher phosphorylation levels in the second-generation, 28z CAR T cells (figure 7D). In contrast, the CD3ζ142 phosphorylation level of EFL28 rTCR-CAR T cells was similar to that of T cells (figure 7D).

To further elucidate the differences observed in vivo, EFL28 rTCR-CAR T cells were phenotypically characterized on repetitive in vitro antigen exposure, with the second-generation 28z CAR T cells as a comparator. After repeated antigen exposure, the EFL28 rTCR-CAR T cells had a higher proportion

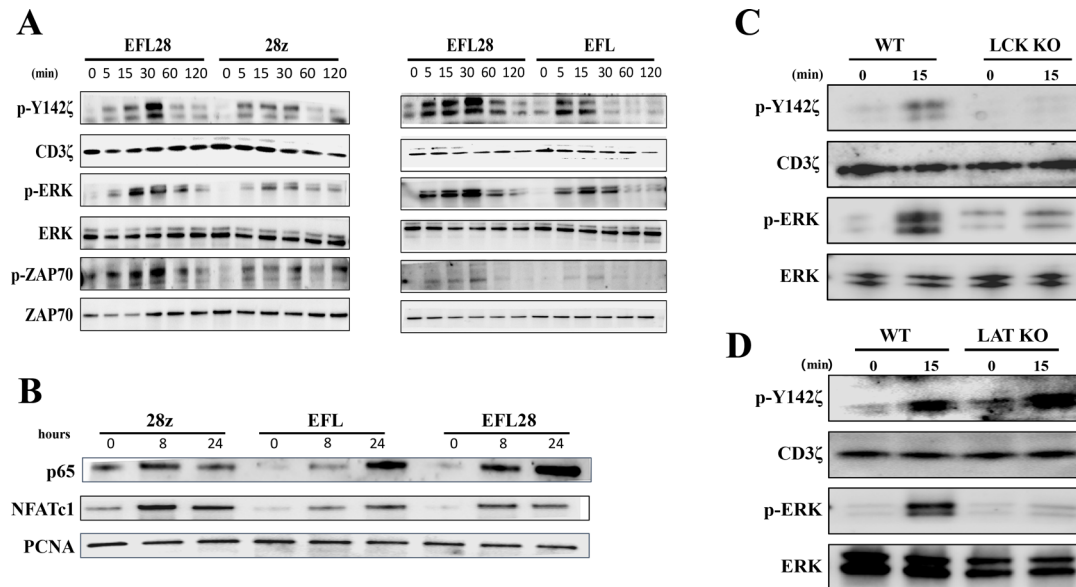


Figure 6 EFL28 receptor-mediated T-cell activation signaling pathway. (A) The effector cells were incubated with 5 μg/mL EDB protein for the indicated times. The phosphorylation levels of CD3ζ, ERK, and ZAP70 and (B) the protein levels of p65 and NFATc1 in whole-cell lysates were detected by Western blotting. (C) Jurkat^{LCK KO} or (D) Jurkat^{LAT KO} cells and wild-type Jurkat cells as controls were transduced with lentivirus to n for the indicated times. The phosphorylation levels of CD3ζ and ERK in whole-cell lysates were detected by Western blotting. EDB, extra domain B.

of naive-like T cells but a lower proportion of effector T cells (figure 7E). The ratio of PD-1-positive, TIM-3-positive, or LAG-3-positive cells in the EFL28 rTCR-CAR T cells was also significantly lower than that in the second-generation, 28z CAR T cells (figure 7F). EFL28 rTCR-CAR T cells exhibited enhanced proliferation and displayed greater cytotoxicity in comparison to the 28z CAR T cells (figure 7G,H). These results indicated that the EFL28 rTCR-CAR T cells maintained a more naive-like and unexhaustive phenotype even on repeated antigen exposure, consistent with their observed superior antitumor efficacy in vivo.

DISCUSSION

Using EDB-fibronectin as a target, we found that the engineered rTCR-CARs with chimeric CD3ε mediated effective in vivo tumor growth inhibition. The eradication of tumors in animal models depended on incorporating the costimulatory domain from CD28 to CD3ε within the rTCR-CAR structure. TCR-based CAR has recently gained more interest among cell-based therapy researchers.^{32 44–46} Our study is the first to observe meaningful eradication of xenograft tumors using EDB-targeting redirected TCR-T cells. Further, the enhanced in vivo activities of the rTCR-CAR EFL28 over the second-generation EDB CAR T cells may be due to increased phosphorylation of the ZAP70, ERK, CD3ζ, and p65 NFκB proteins, as well as highly clustered receptor complexes in rTCR-CAR T cells. In addition, the EFL28 rTCR-CAR T cells had less tonic signaling in the quiescent state without antigen stimulation and were less exhausted on multiple stimulations. Also, the rTCR-CAR T cells possessed a more naive-like phenotype in the quiescent state and were activated

in a mechanism similar to that of TCR. rTCR-CAR design could be applied to other immobile antigens, leading to additional CAR T-cell-based therapies.

Small tumors in the xenograft model have incomplete barriers for immune cell infiltration and therefore lack a suppressive TME, and tumors with sizes exceeding 100 mm³ are considered established with a suppressive TME.⁴² Yet, we still observed significant tumor growth retardation by rTCR-CAR T cells (figure 3F). Further, large tumors formed by an EDB knockout cell line were also inhibited. EDB CAR T cells were cytotoxic to endothelial cells retrieved from the EDB knockout tumor tissues. Thus, efficacious targeting by using EDB CAR T cells in large tumors was probably due to the disruption of the endothelium layer. By targeting the EDB-fibronectin, the CAR T cells can selectively inhibit the growth of the new blood vessels in the tumor, depriving the tumor cells of vital nutrients and oxygen. The EDB-targeting CAR T cells do not need to penetrate the TME to achieve their antiangiogenic effects. This approach is distinct from conventional CAR T cells, which typically target antigens expressed on the tumor cells and must enter the TME to be effective. This unique feature makes EDB CAR an attractive candidate for developing efficacious and safe cancer therapies. A summary of CAR targeting endothelial cells for tumor treatment was provided in a recent review.⁴⁷ However, our study is the first to show that tumor endothelial cells can be effectively, safely, and specifically targeted by CAR T cells. Earlier, CAR T cells targeting VEGFR-2 or VEGFR-1 inhibited the growth of vascularized syngeneic tumors or xenograft models in mice.^{48 49} This approach used a second-generation CAR and required IL-2

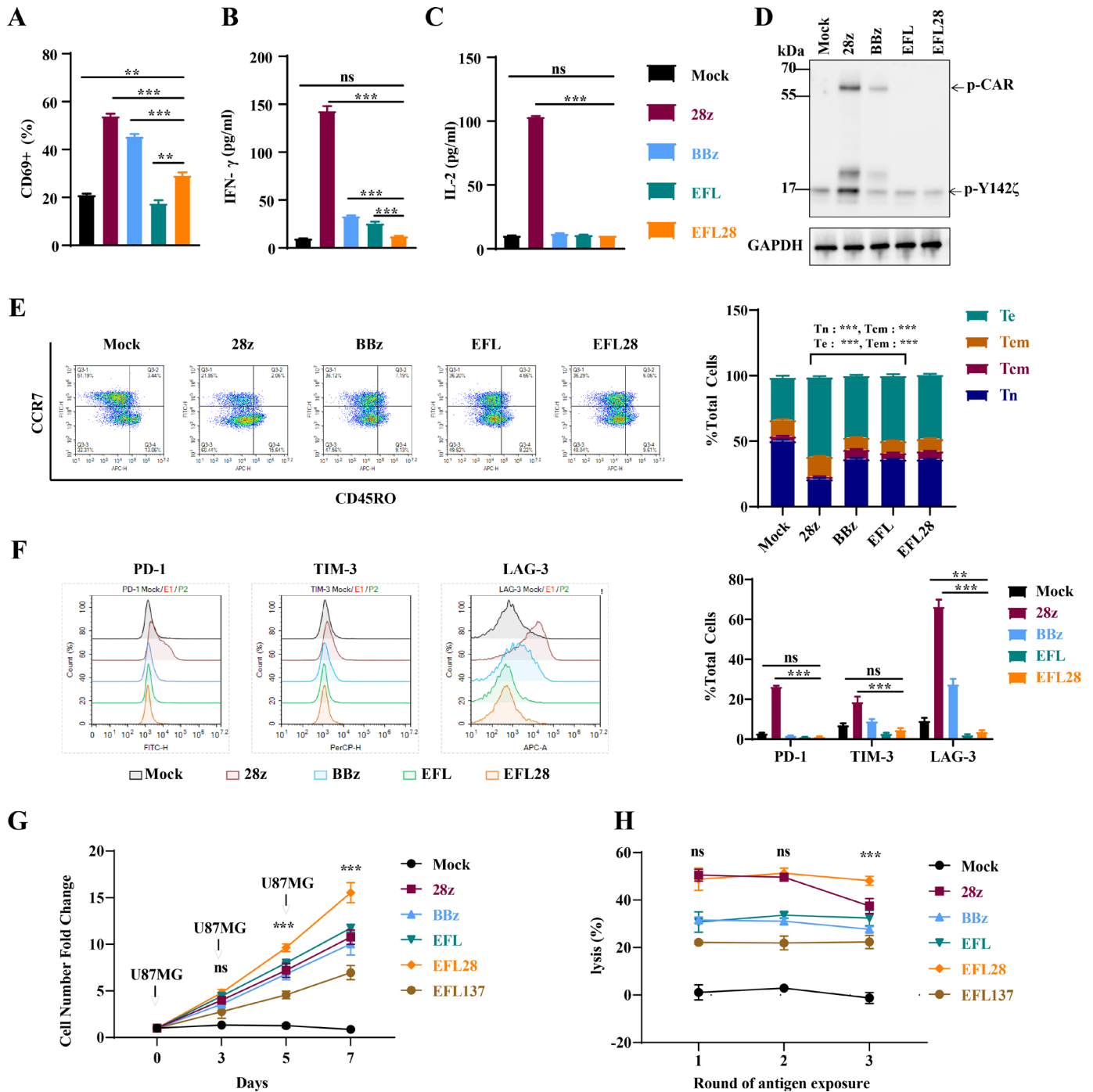


Figure 7 Differences between second-generation CAR and chimeric rTCR-CAR T cells. (A–D) Primary human T cells were transduced with lentivirus to obtain effector cells expressing CARs, and T cells were transduced with the empty virus to obtain control cells. (A) Cells were cultured without antigen exposure for 14 days. The positive rate of CD69 in each group was detected by flow cytometry (n=3). (B C) Expression levels of IFN- γ and IL-2 were detected by ELISA, n=3. (D) Cell proteins were extracted from each group, and the phosphorylation level of CD3 ζ was detected by Western blot. (E) The differentiation and (F) exhaustion of CAR T cells in each group without antigen stimulation were detected by flow cytometry, n=3. (G) Proliferation of CAR-T cells with repeated antigen stimulation, n=3. (H) Cytotoxicity of CAR-T cells after 1, 2, or 3 times of antigen exposure, n=3. Statistical significance was calculated by one-way analysis of variance with Bonferroni post hoc test, **p<0.01, ***p<0.001. CAR, chimeric antigen receptor.

supplementation or coexpression of IL-15 for in vivo efficacy and failed to produce objective responses in the clinical trial (NCT01218867). EDB-fibronectin is required for endothelial cell attachment during angiogenesis.⁵⁰ Thus,

targeting EDB-fibronectin using EDB rTCR-CAR T cells may be a significant breakthrough in anti-angiogenic therapies.

Further, disruption of tumor neovasculature might be used as a base for combination therapies, in which therapeutic agents with poor penetration into tumor tissue can achieve greater efficacy once the vasculature is disrupted. Combination with oncolytic viruses can also be considered since many oncolytic viruses require intratumor injections to be effective. Other CARs targeting a different tumor antigen could be combined with the EDB-targeting rTCR-CAR to achieve more significant tumor killing at the site of disrupted neovasculature.

We noticed that the rTCR-CAR T cells disappeared after 28 days *in vivo*, suggesting that EDB-fibronectin on endothelial cells is no longer available or abundant enough to maintain the dividing pool of T cells. The lack of persistence might also be due to activation-induced cell death and contraction of the CAR T-cell pool after exhaustion.¹⁰ We did not inject extraneous IL-2 into the mice to maintain the infused CAR T cells. Additional tests using murine CAR T cells and immune-competent mice are required to identify the causes of CAR T-cell contraction. In our laboratory, we noticed that fortifying rTCR-CAR T cells with constitutively active IL-7 signaling⁵¹ did not drive T cells' *in vivo* expansion and persistence (unpublished). However, developing IL-2 receptor variants that promote IL-2-independent proliferation in activated T cells represents a viable strategy for enhancing the sustained efficacy of CAR-T cell therapy.

EDB-containing fibronectin is likely a docking site for cell attachment to the extracellular matrix.^{50,52} Therefore, the extracellular matrix with EDB-fibronectin may function as a track for migrating cancer cells or endothelial cells.^{53–55} This model is consistent with the findings that mice lacking EDA and EDB-fibronectin demonstrated collapsed microtubes consisting of endothelial cells¹⁹ or with expression levels proportional to the degrees of malignancy.^{56–59} EDB-fibronectin is typically absent from the resting endothelium of healthy tissues; thus, targeting EDB-fibronectin for cancer treatment may be devoid of on-target off-tumor toxicities. Nevertheless, the EDB rTCR-CAR T cells bind to and are cytotoxic to murine endothelial cells expressing EDB-fibronectin. However, our study found no destruction or any form of inflammatory infiltration caused by EDB rTCR-CAR T cells in normal tissues, suggesting that targeting EDB-fibronectin may have fewer side effects than other anti-angiogenic therapies that may also target normal vasculature. Thus, targeting EDB-fibronectin by rTCR-CAR T cells can be a promising approach for treating solid tumors characterized by high neovascularization with limited treatment options, such as sarcoma. This approach warrants further development, notably where other antiangiogenic therapies have failed.

Twitter Meijia Yang @MeijiaY

Contributors ZZ: method development, experimentation, data analysis, and manuscript preparation and modifications; CL, MW, RS, ZY, YW and MW: experimentation and data analysis; HW and WQ: data analysis; HY: experimentation guidance, data analysis and reviewing; MY: concept, validation, writing, and editing.

MY accepts full responsibility for the work and the conduct of the study, had access to the data, and controlled the decision to publish.

Funding Jiangsu Cell Tech Medical Research Institute funded the study.

Competing interests MY, ZZ and HY are inventors for a patent related to the EDB-targeting T-cell therapies. MY and HY are shareholders of Jiangsu Cell Tech Medical Research Institute. Other authors declare no conflict of interest.

Patient consent for publication Not applicable.

Ethics approval The Institutional Animal Care and Use Committee of China Pharmaceutical University reviewed and approved all experimental animal protocols with a protocol identification number 2022-02-006.

Provenance and peer review Not commissioned; externally peer reviewed.

Data availability statement Data are available on reasonable request.

Supplemental material This content has been supplied by the author(s). It has not been vetted by BMJ Publishing Group Limited (BMJ) and may not have been peer-reviewed. Any opinions or recommendations discussed are solely those of the author(s) and are not endorsed by BMJ. BMJ disclaims all liability and responsibility arising from any reliance placed on the content. Where the content includes any translated material, BMJ does not warrant the accuracy and reliability of the translations (including but not limited to local regulations, clinical guidelines, terminology, drug names and drug dosages), and is not responsible for any error and/or omissions arising from translation and adaptation or otherwise.

Open access This is an open access article distributed in accordance with the Creative Commons Attribution Non Commercial (CC BY-NC 4.0) license, which permits others to distribute, remix, adapt, build upon this work non-commercially, and license their derivative works on different terms, provided the original work is properly cited, appropriate credit is given, any changes made indicated, and the use is non-commercial. See <http://creativecommons.org/licenses/by-nc/4.0/>.

ORCID iD

Meijia Yang <http://orcid.org/0009-0000-8928-5249>

REFERENCES

- Marofi F, Motavalli R, Safonov VA, *et al.* CAR T cells in solid tumors: challenges and opportunities. *Stem Cell Res Ther* 2021;12.
- Patel U, Abernathy J, Savani BN, *et al.* CAR T cell therapy in solid tumors: A review of current clinical trials. *EJHaem* 2022;3:24–31.
- Hou B, Tang Y, Li W, *et al.* Efficiency of CAR-T therapy for treatment of solid tumor in clinical trials: A meta-analysis. *Dis Markers* 2019;2019:3425291.
- Grigor EJM, Fergusson D, Kekre N, *et al.* Risks and benefits of chimeric antigen receptor T-cell (CAR-T) therapy in cancer: a systematic review and meta-analysis. *Transfus Med Rev* 2019;33:98–110.
- Parkhurst MR, Yang JC, Langan RC, *et al.* T cells targeting carcinoembryonic antigen can mediate regression of metastatic colorectal cancer but induce severe transient colitis. *Mol Ther* 2011;19:620–6.
- Morgan RA, Yang JC, Kitano M, *et al.* Case report of a serious adverse event following the administration of T cells Transduced with a Chimeric antigen receptor recognizing ErbB2. *Mol Ther* 2010;18:843–51.
- Lamers CHJ, Sleijfer S, Vulto AG, *et al.* Treatment of metastatic renal cell carcinoma with autologous T-lymphocytes genetically retargeted against carbonic anhydrase IX: first clinical experience. *J Clin Oncol* 2006;24:e20–2.
- Rodríguez-García A, Palazon A, Noguera-Ortega E, *et al.* CAR-T cells hit the tumor microenvironment: strategies to overcome tumor escape. *Front Immunol* 2020;11:1109.
- Martinez M, Moon EK. CAR T cells for solid tumors: new strategies for finding, infiltrating, and surviving in the tumor Microenvironment. *Front Immunol* 2019;10:128.
- McLellan AD, Ali Hosseini Rad SM. Chimeric antigen receptor T cell persistence and memory cell formation. *Immunol Cell Biol* 2019;97:664–74.
- Qi C, Gong J, Li J, *et al.* Claudin18.2-specific CAR T cells in gastrointestinal cancers: phase 1 trial interim results. *Nat Med* 2022;28:1189–98.
- Zhang Q, Hresko ME, Picton LK, *et al.* A human orthogonal IL-2 and IL-2Rβ system enhances CAR T cell expansion and antitumor activity in a murine model of leukemia. *Sci Transl Med* 2021;13:eabg6986.
- Kagoya Y, Tanaka S, Guo T, *et al.* A novel chimeric antigen receptor containing a JAK–STAT signaling domain mediates superior antitumor effects. *Nat Med* 2018;24:352–9.



- 14 Hawkins ER, D'Souza RR, Klampatsa A. Armored CAR T-cells: the next chapter in T-cell cancer immunotherapy. *Biologics* 2021;15:95–105.
- 15 Kato D, Yaguchi T, Iwata T, et al. Gpc1 specific CAR-T cells eradicate established solid tumor without adverse effects and synergize with anti-PD-1 AB. *Elife* 2020;9:e49392.
- 16 Heczey A, Louis CU, Savoldo B, et al. CAR T cells administered in combination with lymphodepletion and PD-1 inhibition to patients with neuroblastoma. *Mol Ther* 2017;25:2214–24.
- 17 Ma L, Dichwalkar T, Chang JYH, et al. Enhanced CAR-T cell activity against solid tumors by vaccine boosting through the chimeric receptor. *Science* 2019;365:162–8.
- 18 Reinhard K, Rengstl B, Oehm P, et al. An RNA vaccine drives expansion and efficacy of claudin-CAR-T cells against solid tumors. *Science* 2020;367:446–53.
- 19 Astrof S, Crowley D, Hynes RO. Multiple cardiovascular defects caused by the absence of alternatively spliced segments of fibronectin. *Dev Biol* 2007;311:11–24.
- 20 Carnemolla B, Neri D, Castellani P, et al. Phage antibodies with pan-species recognition of the oncofetal angiogenesis marker fibronectin ED-B domain. *Int J Cancer* 1996;68:397–405.
- 21 Castellani P, Viale G, Dorcaratto A, et al. The fibronectin Isoform containing the Ed-B oncofetal domain: a marker of angiogenesis. *Int J Cancer* 1994;59:612–8.
- 22 Kaczmarek J, Castellani P, Nicolo G, et al. Distribution of oncofetal fibronectin Isoforms in normal, hyperplastic and neoplastic human breast tissues. *Int J Cancer* 1994;59:11–6.
- 23 Neri D, Bicknell R. Tumour vascular targeting. *Nat Rev Cancer* 2005;5:436–46.
- 24 Wagner J, Wickman E, Shaw TI, et al. Antitumor effects of CAR T cells redirected to the EDB splice variant of fibronectin. *Cancer Immunol Res* 2021;9:279–90.
- 25 Xie YJ, Dougan M, Jailkhani N, et al. Nanobody-based CAR T cells that target the tumor microenvironment inhibit the growth of solid tumors in immunocompetent mice. *Proc Natl Acad Sci USA* 2019;116:7624–31.
- 26 Khan ZA, Chan BM, Uniyal S, et al. EDB fibronectin and angiogenesis—a novel mechanistic pathway. *Angiogenesis* 2005;8:183–96.
- 27 Birchler MT, Milisavljevic D, Pfaltz M, et al. Expression of the extra domain B of fibronectin, a marker of angiogenesis, in head and neck tumors. *Laryngoscope* 2003;113:1231–7.
- 28 Castellani P, Borsi L, Carnemolla B, et al. Differentiation between high- and low-grade astrocytoma using a human recombinant antibody to the extra domain-B of fibronectin. *Am J Pathol* 2002;161:1695–700.
- 29 Midulla M, Verma R, Pignatelli M, et al. Source of Oncofetal ED-B-containing fibronectin: implications of production by both tumor and endothelial Cells1. *Cancer Res* 2000;60:164–9.
- 30 Gilham DE, O'Neil A, Hughes C, et al. Primary polyclonal human T lymphocytes targeted to carcino-embryonic antigens and neural cell adhesion molecule tumor antigens by Cd3Z-based chimeric immune receptors. *J Immunother* 2002;25:139–51.
- 31 Bridgeman JS, Hawkins RE, Bagley S, et al. The optimal antigen response of chimeric antigen receptors harboring the Cd3Z. Transmembrane domain is dependent upon incorporation of the receptor into the endogenous TCR/Cd3 complex. *J Immunol* 2010;184:6938–49.
- 32 Baeuerle PA, Ding J, Patel E, et al. Synthetic trunc receptors engaging the complete T cell receptor for potent anti-tumor response. *Nat Commun* 2019;10:2087.
- 33 Pini A, Viti F, Santucci A, et al. Design and use of a phage display library. human antibodies with subnanomolar affinity against a marker of angiogenesis eluted from a two-dimensional gel. *J Biol Chem* 1998;273:21769–76.
- 34 Zhang Z, Liu C, Yang Z, et al. CAR-T-cell therapy for solid tumors positive for fibronectin extra domain B. *Cells* 2022;11:2863.
- 35 D'Ovidio MC, Mastracchio A, Marzullo A, et al. Intratumoral microvessel density and expression of ED-A/ED-B sequences of fibronectin in breast carcinoma. *Eur J Cancer* 1998;34:1081–5.
- 36 Sauer S, Erba PA, Petrini M, et al. Expression of the oncofetal ED-B-containing fibronectin Isoform in hematologic tumors enables ED-B-targeted 131I-L19Sip radioimmunotherapy in hodgkin lymphoma patients. *Blood* 2009;113:2265–74.
- 37 Hall C, Berkhout B, Alarcon B, et al. Requirements for cell surface expression of the human TCR/Cd3 complex in non-T cells. *Int Immunol* 1991;3:359–68.
- 38 Kappes DJ, Tonegawa S. Surface expression of alternative forms of the TCR/Cd3 complex. *Proc Natl Acad Sci U S A* 1991;88:10619–23.
- 39 Yokosuka T, Saito T. Dynamic regulation of T-cell costimulation through TCR–Cd28 microclusters. *Immunol Rev* 2009;229:27–40.
- 40 Davenport AJ, Cross RS, Watson KA, et al. Chimeric antigen receptor T cells form nonclassical and potent immune synapses driving rapid cytotoxicity. *Proc Natl Acad Sci USA* 2018;115:E2068–76.
- 41 Xiong W, Chen Y, Kang X, et al. Immunological synapse predicts effectiveness of chimeric antigen receptor cells. *Mol Ther* 2018;26:963–75.
- 42 Yu P, Rowley DA, Fu Y-X, et al. The role of stroma in immune recognition and destruction of well-established solid tumors. *Curr Opin Immunol* 2006;18:226–31.
- 43 Borsi L, Balza E, Bestagno M, et al. Selective targeting of tumoral vasculature: comparison of different formats of an antibody (L19) to the ED-B domain of fibronectin. *Int J Cancer* 2002;102:75–85.
- 44 Liu Y, Liu G, Wang J, et al. Chimeric STAR receptors using TCR machinery mediate robust responses against solid tumors. *Sci Transl Med* 2021;13:eabb5191.
- 45 Altenschmidt U, Kahl R, Moritz D, et al. Cytolysis of tumor cells expressing the neu/erbB-2, erbB-3, and erbB-4 receptors by genetically targeted naive T lymphocytes. *Clin Cancer Res* 1996;2:1001–8.
- 46 Moritz D, Wels W, Mattern J, et al. Cytotoxic T lymphocytes with a grafted recognition specificity for ErbB2-expressing tumor cells. *Proc Natl Acad Sci U S A* 1994;91:4318–22.
- 47 Akbari P, Katsarou A, Daghighian R, et al. Directing CAR T cells towards the tumor vasculature for the treatment of solid tumors. *Biochimica et Biophysica Acta (BBA) - Reviews on Cancer* 2022;1877:188701.
- 48 Chinnsamy D, Yu Z, Theoret MR, et al. Gene therapy using genetically modified lymphocytes targeting VEGFR-2 inhibits the growth of Vascularized Syngenic tumors in mice. *J Clin Invest* 2010;120:3953–68.
- 49 Wang W, Ma Y, Li J, et al. Specificity redirection by CAR with human VEGFR-1 affinity endows T lymphocytes with tumor-killing ability and anti-angiogenic potency. *Gene Ther* 2013;20:970–8.
- 50 Cseh B, Fernandez-Sauze S, Grall D, et al. Autocrine fibronectin directs matrix assembly and crosstalk between cell-matrix and cell-cell adhesion in vascular endothelial cells. *J Cell Sci* 2010;123:3989–99.
- 51 Shum T, Omer B, Tashiro H, et al. Constitutive signaling from an engineered I17 receptor promotes durable tumor elimination by tumor-redirected T cells. *Cancer Discov* 2017;7:1238–47.
- 52 Hashimoto-Uoshima M, Yan YZ, Schneider G, et al. The alternatively spliced domains EIIIB and EIIIA of human fibronectin affect cell adhesion and spreading. *J Cell Sci* 1997;110 (Pt 18):2271–80.
- 53 Erdogan B, Ao M, White LM, et al. Cancer-associated fibroblasts promote directional cancer cell migration by aligning fibronectin. *J Cell Biol* 2017;216:3799–816.
- 54 Gopal S, Veracini L, Grall D, et al. Fibronectin-guided migration of carcinoma collectives. *Nat Commun* 2017;8:14105.
- 55 Ramos G de O, Bernardi L, Lauxen I, et al. Fibronectin modulates cell adhesion and signaling to promote single cell migration of highly invasive oral squamous cell carcinoma. *PLOS ONE* 2016;11:e0151338.
- 56 Saw PE, Xu X, Kang BR, et al. Extra-domain B of fibronectin as an alternative target for drug delivery and a cancer diagnostic and Prognostic biomarker for malignant glioma. *Theranostics* 2021;11:941–57.
- 57 Lyons AJ, Bateman AC, Spedding A, et al. Oncofetal fibronectin and oral squamous cell carcinoma. *Br J Oral Maxillofac Surg* 2001;39:471–7.
- 58 Mhawech P, Dulguerov P, Assaly M, et al. EB-D fibronectin expression in squamous cell carcinoma of the head and neck. *Oral Oncol* 2005;41:82–8.
- 59 Vaidya A, Wang H, Qian V, et al. Overexpression of extradomain-B fibronectin is associated with invasion of breast cancer cells. *Cells* 2020;9:1826.